0273-2289/03/105-108/0413/$20.00

Hybrid Model for an Enzymatic Reactor

Hydrolysis of Cheese Whey Proteins by Alcalase Immobilized in Agarose Gel Particles

Ruy Sousa Jr., Mariam M. Resende, Raquel L. C. Giordano, and Roberto C. Giordano*

Departamento de Engenharia Química, Universidade Federal de São Carlos, Via Washington Luiz, km 235, CP 676, São Carlos/SP, Brazil 13565-905, E-mail address: roberto@deq.ufscar.br

Abstract

Cheese whey proteolysis, carried out by immobilized enzymes, can either change or evidence functional properties of the produced peptides, increasing the potential applications of this byproduct of the dairy industry. Optimization and scale-up of the enzymatic reactor relies on its mathematical model—a set of mass balance equations, with reaction rates usually given by Michaelis-Menten-like kinetics; no information about the distribution of peptides' molecular sizes is supplied. In this article, a hybrid model of a batch enzymatic reactor is presented, consisting of differential mass balances coupled to a "neural-kinetic model," which provides the molecular weight distributions of the resulting peptides.

Index Entries: Cheese whey proteolysis; enzymatic reactor; hybrid model; mass balance equations; artificial neural networks.

Introduction

Reduction in the discharge of liquid protein residues generated in the food industry process is a relevant concern *(1)*. An interesting possible solution to the problem is the conversion of those residues into market products. Milky whey, arising from cheese manufacture, was considered, for a long time, a product to be discharged. However, its high biologic oxygen demand (35,000 mg/L) *(2)* and the associated treatment cost have turned it into a byproduct of the food industry.

Whey and its products have been increasingly used in a great number of applications such as for the production of creamer for foaming beverages, edible food films, and milk and salt substitutes. On the other hand,

*Author to whom all correspondence and reprint requests should be addressed.

whey protein hydrolysis, carried out by enzymes immobilized in an inert support, can either change or evidence functional properties of the produced peptides, increasing the potential applications of cheese whey. Whey protein hydrolysates can be used as a protein source for individuals with a reduced capacity for digestion, as a food supplement for phenylketonuria patients, in compositions of bioactive peptides free from bitterness, and so on *(3)*.

Usually, the mathematical model of the enzymatic reactor where whey hydrolysis takes place comprises a set of mass balance equations with reaction rates given by Michaelis-Menten-like kinetics *(4–6)*. Following this approach, substrate concentrations are expressed in terms of unspecific variables such as the number of hydrolyzable peptide bonds in the substrate. The drawback of this approach is that it does not supply any information about the peptides' molecular weight distribution along the reaction course. Only after time-consuming, off-line analyses can one determine the detailed product composition.

In this article, a hybrid model of a batch enzymatic reactor is presented, consisting of differential mass balances coupled to a "neural-kinetic model," which can provide the molecular weight distributions of the resulting peptides. In this way, a more detailed description of the state of the system is achieved.

Feedforward multilayer Perceptron (MLP), *(7)* neural networks (NNs) are trained against empirical data *(8)*. For network training, cheese whey was hydrolyzed by alcalase®, multipunctually immobilized in agarose gel particles, at different pH values. A laboratory-scale batch reactor, with pH control, was used. Samples were periodically withdrawn and analyzed via high-performance liquid chromatography (HPLC). The trained artificial NNs were directly coupled to mass balance equations.

Materials and Methods

Four batch hydrolysis assays were carried out, at different pHs, in a 50-mL jacketed vessel with pH (Metrohm® 718 Stat Titrino) and temperature (thermostatic bath Neslab®) control. The operation temperature was 50°C. Reaction pHs were 7.0, 8.0, 9.0 and 10.0. For each experiment, 30 mL of cheese whey at a nominal concentration of 60 g/L (according to the Kjeldhal method *[9]*) and 0.3 g of agarose gel containing 13.4 U_{BAEE}/g_{gel} were used. One U_{BAEE} corresponds to the quantity of alcalase that hydrolyzes 1 µmol of benzoil arginine ester etilic/min at pH 8.0 and 25°C.

During each assay, free-of-enzyme samples containing 300 µL of hydrolyzed whey were taken. These samples, after properly diluted (15X) were analyzed via size-exclusion chromatography *(9)* (with 0.25 *M* NaCl in 0.02 *M* phosphate buffer, pH 7.2; flow rate of 4.17×10^{-9} m^3/s and detection at 214 nm).

The results of this chromatography analysis were used for training feedforward MLP NNs. For network learning, the "back-propagation"

Table 1
HPLC Standards for Evaluation of Molecular Weight Distribution of Peptides

Standard no.	Identification	*MW* (Daltons)	Retention (min)
1	Bovine serum albumin (Sigma, St. Louis, MO)	67,000	30.0
2	β-Lactoglobulin (Sigma)	18,000	33.5
3	Insulin (Biobrás, Montes Claros, Brazil)	5000	44.2
4	Angiotensin II (Asp-Arg-Val-Tyr-Ile-His-Pro-Phe) (Sigma)	1047	65.0
5	Leucine enkephalin (Tyr-Gly-Gly-Phe-Leu) (Sigma)	556	74.1

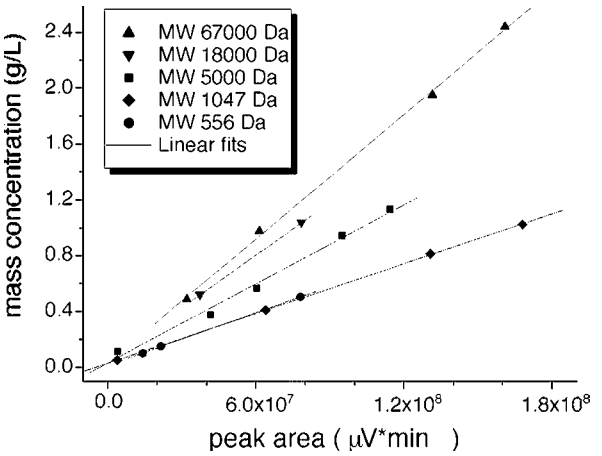

Fig. 1. Calibration curves: mass concentration of standard vs HPLC peak area.

algorithm was used *(10)*. Finally, the classic Runge-Kutta method solved the differential mass balances *(11)*.

Results

Some calibration procedures were necessary for obtaining the peptides' molecular weight distribution for each sample. Initially, five standards were injected into the column (Table 1). Then a calibration curve mass concentration (g/L) vs peak area (μV × min) was built for each standard (Fig. 1).

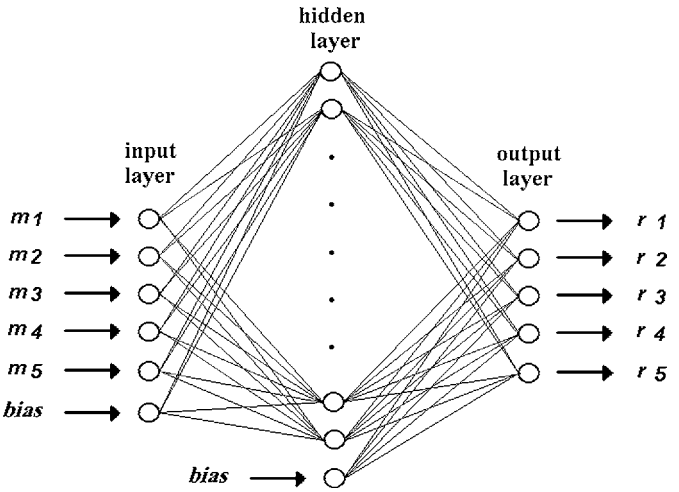

Fig. 2. Feedforward MLP NN.

The linear coefficient of the curves in Fig. 1 was assumed constant and equal to 0.03 g/L ((0 g/L). The slopes, in turn, could be properly fitted as a function of molecular weight (*MW*, Daltons) (Eq. 1):

$$\text{Slope} = -9.14 \times 10^{-9} + 5.03 \times 10^{-9} \log_{10}(MW) \quad (1)$$

Molecular weights could be expressed as a function of the retention time (retention, min) inside the column, as presented in Table 1:

$$\log_{10}(MW) = 5.40 - 0.04 \text{ retention} \quad (2)$$

By combining Eqs. 1 and 2, a general equation was obtained that relates mass concentration (Conc, g/L) to the area in the chromatogram (area, μV × min), as a function of retention time (min):

$$\text{Conc} = 0.03 + \left(-9.14 \times 10^{-9} + 5.03 \times 10^{-9}[5.40 - 0.04 \times \text{retention}]\right) \times \text{area} \quad (3)$$

Through HPLC analysis, it was possible to obtain the peptides' concentrations, for each sample, within five predefined ranges of interest ($MW_1 \leq 650$ Daltons, 650 Daltons $< MW_2 \leq 1050$Da, 1050 Daltons $< MW_3 <$ 4150 Daltons, 4150 Daltons $\leq MW_4 <$ 14,000 Daltons, 14,000 Daltons $\leq MW_5 \leq$ 67,000 Daltons).

Considering each of the five molecular weight ranges as a pseudo-component, feedforward MLP NNs were trained. The NNs were capable of mapping the mass concentrations m_1 ($MW_1 \leq 650$ Daltons), m_2 (650 Daltons $< MW_2 \leq 1050$ Daltons), m_3 (1050 Daltons $< MW_3 <$ 4150 Daltons), m_4 (4150 Daltons $\leq MW_4 <$ 14,000 Daltons) and m_5 (14,000 Daltons $\leq MW_5 \leq$ 67,000 Daltons) into an output vector constituted by the reaction rates of the respective MW ranges, r_1, r_2, r_3, r_4, and r_5.

The feedforward NN (Fig. 2) comprises interconnected layers of processing units (neurons). Processing units in adjacent layers are joined by

Table 2
Mass Concentrations of Each Range
of Peptides' MW (pH 10.0) for Input to NN

m_1 (g/L)	m_2 (g/L)	m_3 (g/L)	m_4 (g/L)	m_5 (g/L)
54.22	0.00	0.00	0.00	0.00
47.44	3.43	1.86	0.88	0.62
34.96	10.46	5.82	1.92	1.06
26.63	13.51	8.17	2.64	3.27
24.17	12.54	8.98	2.97	5.56
20.92[a]	12.41	10.02	3.38	7.50
19.05	12.31	11.06	3.82	7.98
8.20	14.02	14.72	5.41	11.86
5.22	14.17	15.52	6.13	13.19
4.87	12.64	16.37	7.01	13.33
3.77	11.77	16.33	7.60	14.75
2.94	11.32	16.68	8.25	15.03
2.47	10.56	16.57	8.50	16.12

[a]One validation datum point.

weighed connections (w_{ji}). Each unit sums the input weighed signal ($w_{ji}x_i$) and an offset term (a bias w_{jb}).

$$\text{net}_j = \sum_{i=1}^{n} w_{ji} x_i + w_{jb} \tag{4}$$

A nonlinear transfer function (in our case, a sigmoid) evaluates the node output (y_j) using the value of net_j, obtained from Eq. 4:

$$y_j = \frac{1}{1 + \exp\left(-\text{net}_j\right)} \tag{5}$$

The experimental reaction rates r_i were obtained after the direct differentiation of $m_i \times$ time by the proper "calculus tool" of the software Microcal Origin®. Tables 2 and 3 show *typical* data (with experimental and predicted rates). The dispersion of NN learning can be assessed by examining Fig. 3A. Figure 3B shows the dispersion of a validation test using extra data. The numbers of neurons in the hidden layer are 40 (pH 7.0), 45 (pH 8.0), 48 (pH 9.0) and 48 (pH 10.0).

The mass balance equation for the batch stirred-tank reactor (BSTR) is as follows:

$$\frac{d\left(m_i V\right)}{dt} = r_i \rho V \tag{6}$$

in which m_i is mass concentration within range i, V is reactor volume (admitted constant), t is time, r_i is reaction rate supplied by the neural-kinetic model (within range i), and ρ is U_{BAEE}/V.

Table 3
Enzymatic Reaction rates (pH 10.0) for Output of NN

r_1 (g/U_{BAEE}·min)		r_2 (g/U_{BAEE}·min)		r_3 (g/U_{BAEE}·min)		r_4 (g/U_{BAEE}·min)		r_5 (g/U_{BAEE}·min)	
Experimental	NN	Experimental	NN	Experimental	NN	Experimental	NN	Experimental	NN
−0.0759	−0.0759	0.0383	0.0383	0.0208	0.0208	0.0098	0.0098	0.0069	0.0069
−0.0554	−0.0554	0.0290	0.0290	0.0160	0.0160	0.0064	0.0064	0.0041	0.0041
−0.0252	−0.0253	0.0127	0.0127	0.0077	0.0077	0.0021	0.0021	0.0027	0.0027
−0.0093	−0.0093	0.0023	0.0022	0.0027	0.0027	0.0009	0.0009	0.0035	0.0035
−0.0038	−0.0038	−0.0007	−0.0007	0.0012	0.0012	0.0005	0.0005	0.0028	0.0028
−0.0033	−0.0026	−0.0002	−0.0001	0.0013	0.0011	0.0005	0.0005	0.0016	0.0010
−0.0026	−0.0026	0.0002	0.0002	0.0011	0.0011	0.0005	0.0005	0.0008	0.0008
−0.0020	−0.0020	0.0003	0.0003	0.0007	0.0006	0.0003	0.0003	0.0008	0.0008
−0.0005	−0.0005	−0.0002	−0.0001	0.0002	0.0002	0.0002	0.0002	0.0002	0.0002
−0.0001	−0.0002	−0.0002	−0.0002	0.0001	0.0001	0.0001	0.0001	0.0001	0.0001
−0.0001	−0.0001	−0.0001	−0.0001	0.0000	0.0000	0.0001	0.0001	0.0001	0.0001
−0.0001	−0.0001	−0.0001	−0.0001	0.0000	0.0000	0.0001	0.0001	0.0001	0.0001
0.0000	−0.0001	−0.0001	0.0000	0.0000	0.0000	0.0000	0.0000	0.0001	0.0001

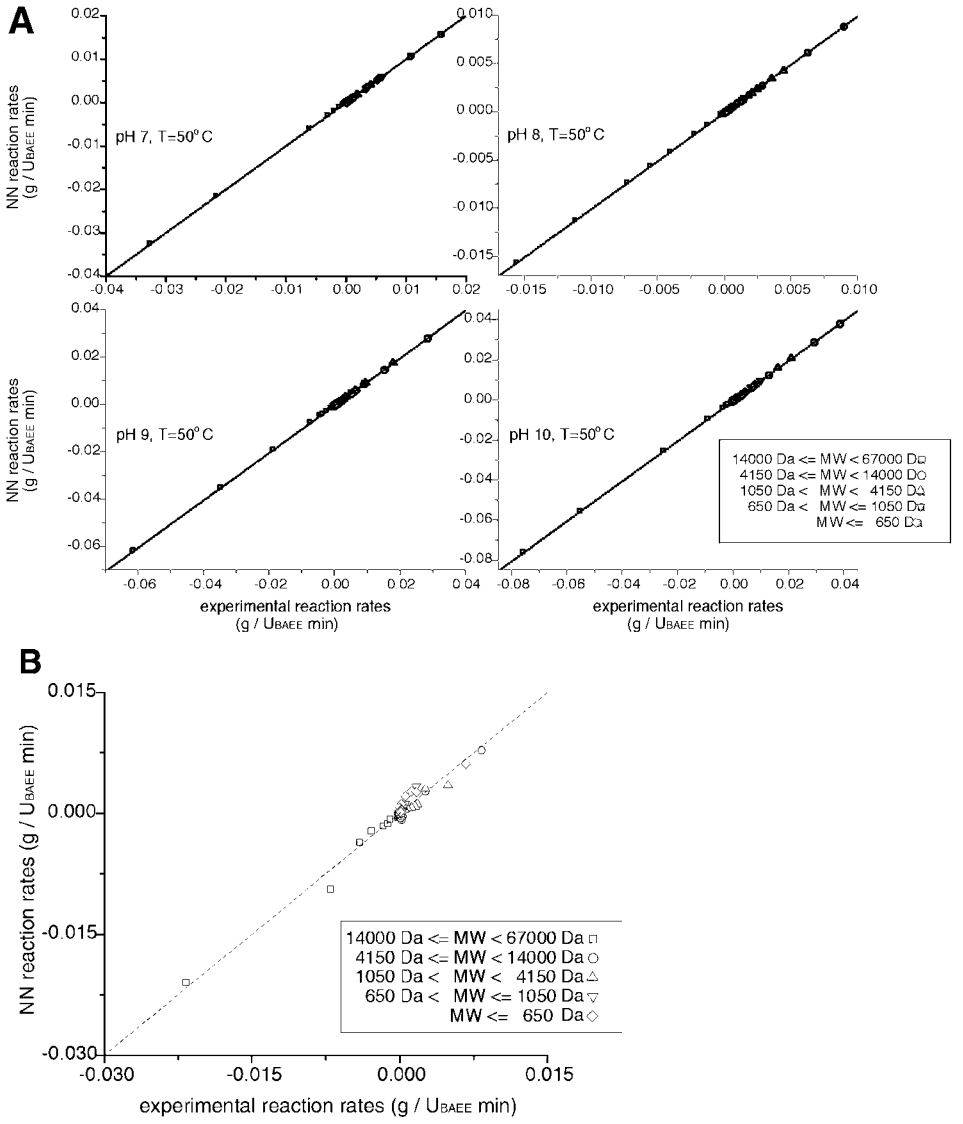

Fig. 3. (**A**) Dispersion of NN learning; (**B**) dispersion in a validation test (pH = 9.0, T = 50°C).

By making use of the classic Runge-Kutta method, the system of ordinary differential equations could be properly solved, providing the hydrolysate composition inside the jacketed BSTR along time. Initial conditions were as follows:

$m_1(0)$ = 63.55 g/L for pH 7.0 assay, 57.78 g/L for pH 8.0 assay, 57.01 g/L for pH 9.0 assay, and 54.22 g/L for pH 10.0 assay; and $m_2(0) = m_3(0) = m_4(0) = m_5(0) = 0$ g/L for all assays.

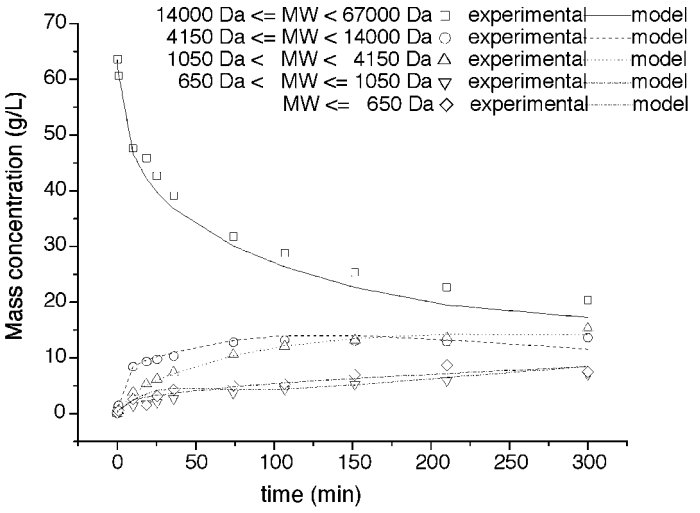

Fig. 4. Distribution of peptides along time (pH = 7.0, T = 50°C).

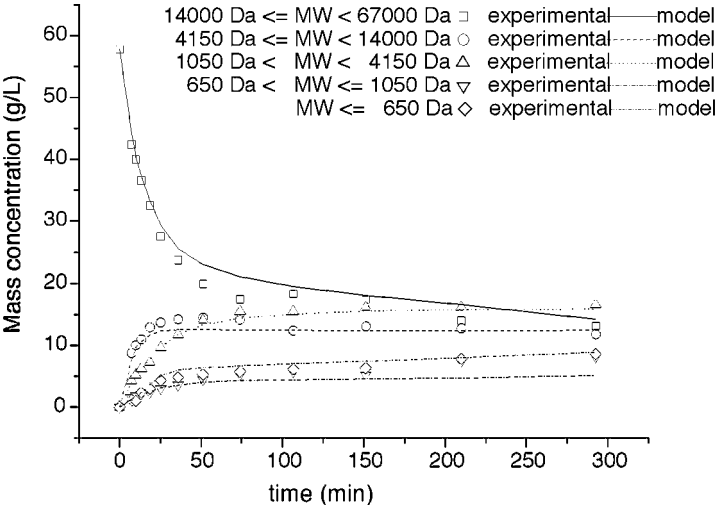

Fig. 5. Distribution of peptides along time (pH = 8.0, T = 50°C).

Note that $m_1(0)$ is not exactly the same for all experiments. The average of the obtained values is 58.14 g/L. This is very close to the nominal cheese whey concentration determined through the Kjeldhal method. Figures 4–7 show the model predictions compared to experimental data, for each of the experimental assays.

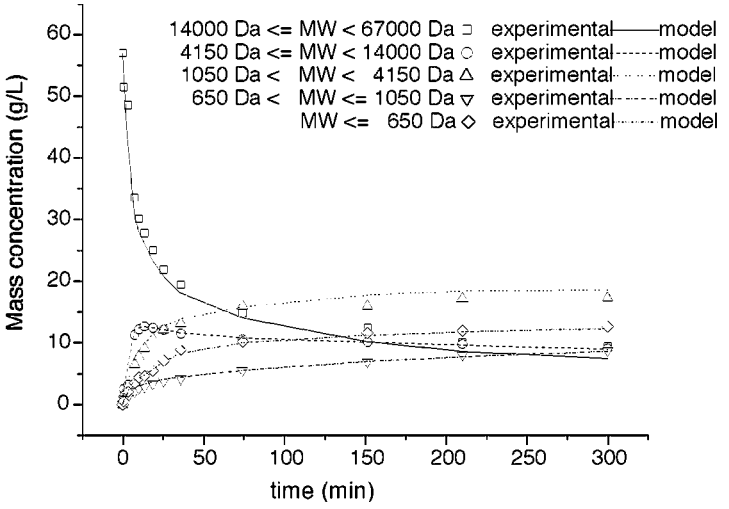

Fig. 6. Distribution of peptides along time (pH = 9.0, T = 50°C).

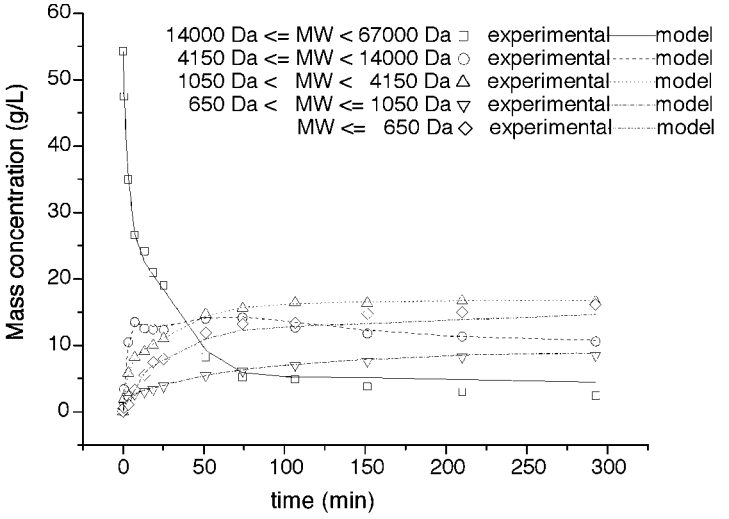

Fig. 7. Distribution of peptides along time (pH = 10.0, T = 50°C).

Discussion

Using HPLC and an appropriate calibration procedure, it was possible to quantify the distribution of peptides' molecular weights along time for different experiments of cheese whey hydrolysis. Feedforward MLP NNs can map accurately the reaction rates as a function of peptides' molecular weight distribution, at different pHs. For intermediary pH e.g., 9.5, it is possible to use direct interpolation.

It was possible to observe that the model predictions for molecular weight distribution of peptides are quite accurate. In this work, the trained NNs were used for simulating the BSTR itself. They can be used for modeling any other kind of reactor utilized in whey enzymatic hydrolysis. In a different work *(12)*, by coupling a reactor modeling presented by Giordano et al. *(13)* and the neural-kinetic model presented here, we built up a hybrid model in order to represent whey proteolysis in a continuous vortex flow reactor. Combining mathematical models with artificial NNs seems to be an important trend in bioprocess modeling *(14–16)*.

Acknowledgments

We thank Fundação de Amparo à Pesquisa do Estado de São Paulo, Conselho Nacional de Desenvolvimento Científico e Tecnológico, Programa de Apoio ao Desenvolvimento Científico e Tecnológico/Conselho Nacional de Desenvolvimento Científico e Tecnológico, and Cooperativa de Lacticínios São Carlos (Brazil).

References

1. Viotto, W. H. (1993), PhD thesis, Unicamp, Campinas, Brazil.
2. Demetrakakes, P. (1997), *Food Processing* **58,** 75–79.
3. Mann, E. (2000), *Dairy Ind. Int.* December, 13–14.
4. Segel, I. H. (1975), Enzyme Kinetics, a Wiley-Interscience, New York, NY.
5. Svendsen, I. (1976), *Carlsberg Res. Commun.* **41,** 237–291.
6. Adler-Nissen, J. (1986), *Enzymic Hydrolysis of Food Proteins*, Elsevier Applied Science, London, England and New York, NY.
7. Scarselli, F. and Tsoi, A. C. (1998), *Neural Networks* **11,** 15–37.
8. Medler, D. A. (1998), *Neural Comput. Surv.* **1,** 61–101.
9. Silvestre, M. P. C. (1997), *Food Chem.* **60,** 263–271.
10. Rumelhart, D. E., Hinton, G. E., and Williams, R. J. (1986), *Nature* **323,** 533–536.
11. Press, W. H., Teukolsky, S. A., Vetterling, W. T., and Flannery, B. P. (1996), *Numerical Recipes in Fortran 90: The Art of Parallel Scientific Computing*, Cambridge University Press, Cambridge, NY.
12. Resende, M. M., Sousa, R., Jr, Tardioli, P. W., Giordano, R. L. C., and Giordano, R. C. (2002), submitted.
13. Giordano, R. C., Giordano, R. L. C., Prazeres, D. M. F., and Cooney, C. L. (2000), *Chem. Eng. Sci.* **55,** 3611–3626.
14. Lübbert, A. and Simutis, R. (1994), *Trends Biotechnol.* **12,** 304–311.
15. Azevedo, S. F., Dahm, B., and Oliveira, F. R. (1997), *Comput. Chem. Eng.* **21,** S751–S756.
16. James, S., Legge, R., and Budman, H. (2002), *J. Process Control* **12,** 113–121.